The Journal of Physiology

https://jp.msubmit.net

JP-RP-2019-278494R2

Title: Incubation with Sodium Nitrite Attenuates Fatigue Development in Intact Single Mouse Fibres at Physiological PO2

Authors: Stephen Bailey
Paulo Guimaraes Gandra
Andrew Jones
Michael Hogan
Leonardo Nogueira

Author Conflict: No competing interests declared

Author Contribution: Stephen Bailey: Conception or design of the work; Acquisition or analysis or interpretation of data for the work; Drafting the work or revising it critically for important intellectual content; Final approval of the version to be published; Agreement to be accountable for all aspects of the work Paulo Guimaraes Gandra: Conception or design of the work; Acquisition or analysis or interpretation of data for the work; Final approval of the version to be published; Agreement to be accountable for all aspects of the work Andrew Jones: Conception or design of the work; Acquisition or analysis or interpretation of data for the work; Drafting the work or revising it critically for important intellectual content; Final approval of the version to be published; Agreement to be accountable for all aspects of the work Michael Hogan: Conception or design of the work; Acquisition or analysis or interpretation of data for the work; Drafting the work or revising it critically for important intellectual content; Final approval of the version to be published; Agreement to be accountable for all aspects of the work Leonardo Nogueira: Conception or design of the work; Acquisition or analysis or

Disclaimer: This is a confidential document.

interpretation of data for the work; Drafting the work or revising it critically for important intellectual content; Final approval of the version to be published; Agreement to be accountable for all aspects of the work

Running Title: Nitrite delays skeletal muscle fatigue at physiological PO2

Dual Publication: No

Funding: Ministry of Science, Technology and Innovation | Conselho Nacional de Desenvolvimento Científico e Tecnológico (National Council for Scientific and Technological Development): Leonardo Nogueira, 424527/2016-2; HHS | NIH | National Institute of Arthritis and Musculoskeletal and Skin Diseases (NIAMS): Michael C Hogan, AR-069577

Disclaimer: This is a confidential document.

Incubation with Sodium Nitrite Attenuates Fatigue Development in Intact Single Mouse Fibres at Physiological P_{O_2}

Stephen J. Bailey[1,2], Paulo G. Gandra[3,4], Andrew M. Jones[1], Michael C. Hogan[3], and Leonardo Nogueira[3,5†]

[1]Sport and Health Sciences, College of Life and Environmental Sciences, University of Exeter, Exeter, UK;
[2]School of Sport, Exercise and Health Sciences, Loughborough University, Loughborough, UK;
[3]Section of Physiology; Division of Pulmonary, Critical Care & Sleep Medicine, Department of Medicine, University of California, San Diego, CA, USA;
[4]Department of Biochemistry and Tissue Biology, Institute of Biology, University of Campinas (Unicamp), Campinas, Brazil.
[5]Instituto de Bioquímica Médica Leopoldo de Meis (Medical Biochemistry Institute Leopoldo de Meis), Federal University of Rio de Janeiro, RJ, Brazil.

Running title: Nitrite delays skeletal muscle fatigue at physiological P_{O_2}.

Key words: Skeletal muscle, muscle fatigue, intracellular calcium, oxygen tension, nitrite anion

Table of Contents category: Skeletal muscle and exercise

[†]Address correspondence to:
Leonardo Nogueira
University of California, San Diego, CA, USA
9500 Gilman Dr. #0623
La Jolla, CA 92093-0623
lnogueira@ucsd.edu

KEY POINTS SUMMARY

- Dietary nitrate supplementation increases plasma nitrite concentration, which provides an oxygen-independent source of nitric oxide and can delay skeletal muscle fatigue.
- Nitrate supplementation has been shown to increase myofibre calcium release and force production in mouse skeletal muscle during contractions at a supra-physiological oxygen tension, but it is unclear whether nitrite exposure can delay fatigue development and improve myofibre calcium handling at a near-physiological oxygen tension.
- Single mouse muscle fibres acutely treated with nitrite had a lower force and cytosolic calcium concentration during single non-fatiguing contractions at a near-physiological oxygen tension.
- Nitrite treatment delayed fatigue development during repeated fatiguing isometric contractions at near-physiological, but not at supra-physiological, oxygen tension in combination with better maintenance of myofilament calcium sensitivity and sarcoplasmic reticulum calcium pumping.
- These findings improve understanding of the mechanisms by which increased skeletal muscle nitrite exposure might be ergogenic and imply that this is related to improved calcium handling.

ABSTRACT

Dietary nitrate (NO_3^-) supplementation, which increases plasma nitrite (NO_2^-) concentration, has been reported to attenuate skeletal muscle fatigue development. Sarcoplasmic reticulum (SR) calcium (Ca^{2+}) release is enhanced in isolated single skeletal muscle fibres following NO_3^- supplementation or NO_2^- incubation at a supra-physiological P_{O_2} but it is unclear whether NO_2^- incubation can alter Ca^{2+} handling and fatigue development at a near-physiological P_{O_2}. We hypothesised that NO_2^- treatment would improve Ca^{2+} handling and delay fatigue at a physiological P_{O_2} in intact single mouse skeletal muscle fibres. Each muscle fibre was perfused with Tyrode's solution pre-equilibrated with either 20% (P_{O_2}~150 Torr) or 2% O_2 (P_{O_2} =15.6 Torr) in the absence and presence of 100 µM $NaNO_2$. At supra-physiological P_{O_2} (i.e., 20% O_2), time to fatigue was lowered by 34% with $NaNO_2$ (control: 257 ± 94 vs. $NaNO_2$: 159 ± 46 s, d=1.63, $P<0.05$), but extended by 21% with $NaNO_2$ at 2% O_2 (control: 308 ± 217 vs. $NaNO_2$: 368 ± 242 s, d=1.14, $P<0.01$). During the fatiguing contraction protocol completed with $NaNO_2$ at 2% O_2, peak cytosolic Ca^{2+} concentration ($[Ca^{2+}]_c$) was not different ($P>0.05$) but $[Ca^{2+}]_c$ accumulation between contractions was lower, concomitant with a greater SR Ca^{2+} pumping rate ($P<0.05$) compared to the control condition. These results demonstrate that increased exposure to NO_2^- blunts fatigue development at near-physiological, but not at supra-physiological, P_{O_2} through enhancing SR Ca^{2+} pumping rate in single skeletal muscle fibres. These findings extend our understanding of the mechanisms by which increased NO_2^- exposure can mitigate skeletal muscle fatigue development.

INTRODUCTION

The gaseous signalling molecule, nitric oxide (NO), was first recognized as an endothelium-derived smooth muscle relaxant (Ignarro *et al*., 1987; Murad *et al*., 1978). However, it is now appreciated that NO can also impact a wide array of physiological processes in skeletal muscle (Stamler and Meissner, 2001; Suhr *et al*., 2013). It is well established that NO can be produced by the NO synthase (NOS) enzymes, which catalyse the five-electron oxidation of L-arginine to NO and L-citrulline (Moncada & Higgs, 1991). More recently, an alternative, O_2-independent pathway for NO generation has been identified in which inorganic nitrate (NO_3^-) can be sequentially reduced to nitrite (NO_2^-) and then to NO (Clanton, 2019; Lundberg & Weitzberg, 2009, 2010). Importantly, dietary supplementation with NO_3^-, which increases circulating plasma [NO_2^-], has been shown to improve skeletal muscle perfusion (Ferguson *et al*., 2013, 2015), contractile and metabolic efficiency (Bailey *et al*., 2010; Fulford *et al*., 2013; Larsen *et al*., 2011; Vanhatalo *et al*., 2011) and contractility (Coggan *et al*., 2015a; Haider & Folland, 2014; Hernández *et al*., 2012; Whitfield *et al*., 2017), and to blunt the development of skeletal muscle fatigue (Bailey *et al*., 2009, 2010; Porcelli *et al*., 2015; Wylie *et al*., 2013).

The chemical reduction of NO_2^- to NO is increased as P_{O_2} (Castello *et al*., 2006) and pH (Modin *et al*., 2001) decline. There is evidence that dietary NO_3^- supplementation is more effective at improving skeletal muscle oxygenation and metabolism and delaying fatigue in hypoxia compared to normoxia (Kelly *et al*., 2014; Vanhatalo *et al*. 2011). Moreover, NO_3^- supplementation increases force production (Hernández *et al*., 2012) and perfusion (Ferguson *et al*., 2013) of fast-twitch (type II) skeletal muscle, which exhibits a lower pH (Tanaka *et al*., 2016) and P_{O_2} (McDonough *et al*., 2005) during contractions, compared to slow-twitch (type I) skeletal muscle. Therefore, the existing evidence suggests that the potential for NO_3^- supplementation to improve skeletal muscle function may depend on intramuscular pH and P_{O_2}.

Although several studies have reported improved exercise economy and/or performance after short-term (3-7 days) (e.g., Bailey *et al*., 2009, 2010; Larsen *et al*., 2007, 2011; Porcelli *et al*., 2015; Whitfield *et al*., 2016) and acute (Wylie *et al*., 2013) dietary NO_3^- supplementation, the mechanisms that underlie these effects remain controversial. For example, short-term NO_3^-

supplementation has been reported to improve exercise economy in association with (Larsen *et al*., 2011), or independently of (Whitfield *et al*., 2016), improved efficiency of mitochondrial oxidative phosphorylation (i.e., a higher P/O ratio). Alternatively, an attenuated high-energy phosphate cost of sub-maximal (Bailey *et al*., 2010) and maximal (Fulford *et al*., 2013) skeletal muscle force production has been observed following short-term NO_3^- supplementation. It is well documented that a significant portion of the energy liberated from high-energy phosphate metabolism is coupled to skeletal muscle Ca^{2+} handling (Barclay, 2015; Walsh et al., 2006). Accordingly, alterations in skeletal muscle Ca^{2+} handling might play an important role in improving skeletal muscle function after NO_3^- ingestion. In line with this postulate, increased tetanic contractile force and cytosolic $[Ca^{2+}]$ ($[Ca^{2+}]_c$) have been observed in single mouse flexor digitorum brevis (FDB) myocytes after short-term (i.e., 7 days) *in vivo* $NaNO_3$ supplementation (Hernández *et al*., 2012). Moreover, $NaNO_3$ supplementation increased tetanic contractile force (Hernández *et al*., 2012) and the content of the Ca^{2+} handling proteins, calsequestrin 1 (CASQ1) and the dihydropyridine receptor (DHPR) in type II extensor digitorum longus muscle, but not in type I soleus muscle (Hernández *et al*., 2012; Ivarsson *et al*., 2017; cf Whitfield *et al*., 2017). Acute exposure to NO_2^- has also been reported to increase $[Ca^{2+}]_c$ in isolated skeletal muscle fibres during tetanic contractions (Andrade *et al*., 1998b). Therefore, alterations in skeletal muscle Ca^{2+} handling appears to play an important role in the improvement in skeletal muscle function after acute and short-term NO_3^- supplementation.

Given that skeletal muscle fatigue and perturbations to Ca^{2+} handling appear to develop in synchrony (Allen *et al*., 2008; Westerblad & Allen, 1994), improved Ca^{2+} handling after NO_3^- or NO_2^- treatment (Andrade *et al*., 1998b; Hernández *et al*., 2012) might be expected to delay skeletal muscle fatigue. However, it has yet to be determined whether acutely exposing skeletal muscle fibres to NO_2^- can abate fatigue development, and to what extent this might be attributable to alterations in Ca^{2+} handling, during repeated tetanic contractions. A limitation of previous experiments assessing the effects of NO_3^- and NO_2^- administration on skeletal muscle force production and Ca^{2+} dynamics is the high experimental P_{O_2} (95% O_2) of the perfusate employed in these studies (Andrade *et al*., 1998b; Hernández *et al*., 2012). This is important because the intracellular P_{O_2} in muscle fibres during intense skeletal muscle contractions is lowered from ~5% O_2 (~30 Torr) to ~ 0.5% O_2 (~2-5 Torr) (Hirai *et al*. 2018; Richardson *et al*.,

1995), and there is evidence that the effects of NO on skeletal muscle contractility and $[Ca^{2+}]_c$ is influenced by the P_{O_2} (Eu *et al*., 2003). Accordingly, further research is required to assess the effects of NO_2^- administration on skeletal muscle contractility, fatigue and $[Ca^{2+}]_c$ at a P_{O_2} that better reflects that which is manifest *in vivo* during intense contractions.

The purpose of the present study was to assess the effects of acute NO_2^- administration on Ca^{2+} handling, evoked force and fatigue resistance in single intact mouse FDB myocytes at both a near-physiological P_{O_2} and the more commonly used supra-physiological P_{O_2}. The single muscle fibre model utilised in the current study also allowed us to isolate the effects of NO_2^- administration on intramyocyte processes in the absence of altered extramyocyte processes such as perfusion. We hypothesized that skeletal muscle Ca^{2+} handling and contractility would be improved, and fatigue development would be delayed, in FDB fibres after NO_2^- incubation at a physiological, but not a supra-physiological, P_{O_2}.

METHODS

Ethical approval

All procedures were approved by the University of California, San Diego Institutional Animal Care and Use Committee (UCSD-IACUC). The experiments in the present investigation comply with *The Journal of Physiology* policy for animal studies, as described by Drummond (2009). Adult male mice (12-16 weeks old; C57BL/6J; The Jackson Laboratory, Bar Harbor, ME; a total of 22 mice were utilized in the present study) were allowed access to water and food *ad libitum*, and were euthanized by an intraperitoneal overdose of sodium pentobarbital (sleep-away; 150 mg/kg). Death was confirmed by absence of movement, heartbeat, and response to toe pinching followed by rapid cervical dislocation to ensure euthanasia.

Single mouse fibre isolation

After euthanasia, the FDB muscles from both posterior feet were quickly excised and individual, intact single muscle fibres (total of 28 fibres used in this study) were microdissected from the whole muscle and transferred to an intact muscle fibre system (model 1500A with force transducer model 403A, Aurora Scientific Inc., Aurora, ON, Canada), as described previously (Nogueira et al., 2018). The intact muscle fibre system was placed on the stage of a Nikon inverted microscope with a 40x long distance Fluor objective. During the experimental procedures, fibres were superfused with Tyrode's solution [in mM: 121 NaCl, 5 KCl, 1.8 $CaCl_2$, 0.5 $MgCl_2$, 0.4 NaH_2PO_4, 24 $NaHCO_3$, 5.5 glucose and 0.1 K_2EGTA, constantly bubbled with 5% CO_2 (for solution pH 7.4) and either 20% O_2 or 2% O_2 as described below]. All experimental procedures were performed at 22ºC.

Isometric force measurements and experimental protocol

Isolated single mouse fibres were electrically stimulated using a Grass S88X stimulator (Quincy, MA) and signal was acquired and analysed as described previously (Gandra et al., 2018). Force development (in mN) was normalized to the cross-sectional area (in mm^2) determined from the diameter of the fibre (32.8 ± 1.4 µm diameter; n=22 fibres, mean ± SE). After being mounted into an experimental chamber, fibres were loaded or injected with the respective fluorescent probe (BCECF-AM or FURA-2) or not treated with any fluorescent probe (as described above).

All fibres underwent a 30 min of constant superperfusion with Tyrode´s solution bubbled with 20% O_2, 5% CO_2 (for extracellular pH 7.4), and N_2 balance followed by electrical stimulations to evoke contractions. Fibre length was then adjusted to achieve optimal isometric tetanic force at 100 Hz (350 ms trains, 0.5 ms pulses, 8 V; L_0). Thereafter, fibres rested for a further 30 min in constant superperfusion with Tyrode´s solution bubbled with either 20% O_2 (for extracellular P_{O_2} of ~156 Torr) or 2% O_2 (for extracellular P_{O_2} of 15.6 ± 0.01 Torr, mean ± SE). The chamber was sealed with a glass cover slip in order to maintain the oxygen tension for the experimental protocol. Oxygen tension of the solution was measured using a needle-type housing fibre optic oxygen microsensor (OXYMICRO, World Precision Instruments, Sarasota, FL) immersed in the experimental chamber solution.

Initially, all fibres were electrically stimulated at different frequencies of pulse stimulation (force-frequency curve; FF; 1-150 Hz; 100 s rest between trains, FF#1). After 5 min of rest, fibres completed a fatigue-inducing contraction protocol (Fatigue #1) comprising a series of 100 Hz trains with the stimulation frequency increased every 2 min (0.25, 0.3, 0.36, 0.43, 0.52, 0.62, 0.75, 0.9, 1.1 trains/s) until task failure, which was defined as the time required for force to decrease by 50%. Immediately following task failure (control), the fibre was superperfused with a 100 µM $NaNO_2$ solution solubilized in Tyrode´s (or modified Tyrode´s when pH_i was measured, see below) and allowed to recover for 60 min. Subsequently, the FF and fatiguing contraction protocols described above were repeated (FF#2 and Fatigue #2, respectively). A schematic of the experimental protocol is presented in Figure 1. In experiments performed on fibres microinjected with FURA-2, the chamber was switched to a Tyrode´s solution containing 10 mM caffeine immediately following the last train of the FF curve and fatigue to evoke a single 120 Hz train and 100 Hz trains, respectively. The concentration of $NaNO_2$ was chosen based on the study of Andrade *et al.*, 1998b, who reported alterations in skeletal muscle force and calcium handling in intact single mouse fibres at non-fatiguing conditions in hyperoxia.

Intracellular Ca^{2+} and pH assessment during contraction

Cytosolic calcium concentration ($[Ca^{2+}]_c$) and intracellular pH (pH_i) changes were obtained by fluorescence spectroscopy using a Photon Technology International illumination and detection system (DeltaScan model) (Nogueira *et al.*, 2018).

$[Ca^{2+}]_c$ measurements

Single muscle fibres (n=5) were pressure injected using a micropipette filled with the ratiometric compound, FURA-2 (Life technologies, Carlsbad, CA, USA; 12 mM, diluted in 150 mM KCl and 10 mM HEPES pH 7.0), followed by 1 h of rest, and subsequent measurement of $[Ca^{2+}]_c$ as described previously (Gandra et al., 2018). Fluorescence excitation ratio (340/380 nm; *R*) was converted to $[Ca^{2+}]_c$ according to equation 1.

$$[Ca^{2+}]_c = K_D \bullet \beta \bullet [(R - R_{min})/(R_{max} - R)] \qquad \text{Eq.1}$$

From equation 1, K_D is the dissociation constant for Ca^{2+}-FURA-2, which was set to 224 nM (Westerblad & Allen, 1991); β (4.51 ± 0.64; n=5 fibres, mean ± SE) is the fluorescence ratio between high and no $[Ca^{2+}]_c$ at 380 nm and was determined for each of the contracting fibres as described previously (Bakker *et al.*, 1993; Andrade *et al.*, 1998a); R_{min} (0.24 ± 0.02; mean ± SE) and R_{max} (5.03 ± 0.84; mean ± SE) are the fluorescence ratios at no cytosolic Ca^{2+} and high Ca^{2+}, respectively, and were determined using an internal *in vivo* calibration described by Gandra *et al*. (2018).

The contraction-induced $[Ca^{2+}]_c$ was calculated by averaging the $[Ca^{2+}]_c$ signal in the final 100 ms of stimulation and subsequently used to determine peak $[Ca^{2+}]_c$. The $[Ca^{2+}]_c$ before each contraction (i.e, basal $[Ca^{2+}]_c$) was calculated by averaging the signal in the 100 ms preceding each stimulation. To determine myofilament Ca^{2+} sensitivity, force development data at each peak $[Ca^{2+}]_c$ during the force-frequency (FF) curves were fitted with a sigmoidal equation (Gandra *et al*., 2018) described in equation 2:

$$P = P_{min} + [(P_0 \bullet [Ca^{2+}]_c^{\,n})/(Ca^{2+}_{50}{}^{n} + [Ca^{2+}]_c^{\,n})] \qquad \text{Eq.2}$$

From equation 2, P is the force developed at different $[Ca^{2+}]_c$, P_0 is the maximal force development, P_{min} is the minimum force developed, Ca^{2+}_{50} is the midpoint of the force-$[Ca^{2+}]_c$ curve, and *n* is nH, the Hill coefficient.

To determine whether fatiguing contractions altered myofilament Ca^{2+} sensitivity, force development data during the fatigue-inducing contraction protocol were plotted at each peak $[Ca^{2+}]_c$ and fitted with equation 2 to determine Ca^{2+}_{50} during fatigue. However, the first 40 s of contractions were not used to determine Ca^{2+}_{50} since they represent the phase 1 of fatigue (Westerblad & Allen, 1991).

During the contraction protocols, SR Ca^{2+} pumping was measured using the procedures described by (Nogueira et al. 2018). Briefly, a SR Ca^{2+} pumping curve was obtained by plotting the rate of $[Ca^{2+}]_c$ decline ($-d[Ca^{2+}]c/dt$) during the elevated long tail of $[Ca^{2+}]_c$ decay (from 100 ms – 3 s after the stimulation period) versus $[Ca^{2+}]_c$ (Equation 3).

$$-d[Ca^{2+}]_c/dt = A \bullet [Ca^{2+}]_c^{N} - L \qquad \text{Eq.3}$$

From equation 3, *A*, *N* and *L* are three adjustable parameters representing the rate of SR Ca^{2+} pumping (in $\mu M^{N-1} \cdot s^{-1}$), the power function, and the SR Ca^{2+} leak, respectively. In order to directly compare SR Ca^{2+} pumping (in $\mu M^{-3} \cdot s^{-1}$) between the control and $NaNO_2$ conditions at the same time-points of the fatigue protocols (first contraction, 80 s of contractions, and the point of task failure), the curves were fitted with *N* and *L* fixed at 4 and 30, respectively. These values were based on mean values of 4.4 ± 0.2 for *N* and 32 ± 4 and for *L* obtained in individual experiments (n=5 fibres, mean ± SE), with a maximum increase in least-square error of 15% (Nogueira *et al.*, 2018).

pH_i measurements

Single muscle fibres (n=5) were loaded with 2', 7'-bis-(2-carboxyethyl)-5-(and -6)-carboxyfluorescein (BCECF-AM; Life technologies, Carlsbad, CA, USA; prepared as stock solution of 10 mM in 100% ethanol and diluted in Tyrode´s to final concentration of 10 µM BCECF-AM and 0.1% ethanol) for 30 min at room temperature. After the incubation period, excess BCECF-AM was washed out twice with 10 ml Tyrode´s, followed by a 30 min resting period with constant superperfusion with Tyrode´s. Intracellular pH (pH_i) changes during contractions were performed as described previously (Nogueira *et al.*, 2013). After completing the experimental protocol, each fibre loaded with BCECF-AM underwent an *in vivo* calibration

procedure, involving 20 min incubation in two different pH buffered solutions (175 mM KCl, 1.2 mM KH_2PO_4, 0.5 mM $MgCl_2$, 10 mM HEPES, 10 µM nigericin), previously titrated with KOH to pH 5.0 and 9.0 as the fluorescence signal was detected. To determine the logarithmic dissociation constant (pK_A), another group of fibres (n=3) were loaded with BCECF-AM, incubated for 20 min in each of the 12 different pH buffered solutions (ranging from pH 5.0 to pH 9.0), and the fluorescence signal was detected (Nogueira *et al.*, 2013). To convert the fluorescence signals to pH_i, fluorescence excitation ratio (440/490 nm; F) was then converted to pH_i according to equation 4.

$$pH_i = pK_A - \log [(F - F_b)/(F_a - F)] - \log (S_b/S_a) \qquad \text{Eq. 4}$$

From equation 4, pK_A was set to 7.14 (7.14 ± 0.03, n=3 fibres; mean ± SE). S_b and S_a are the fluorescence signals from 440 nm excitation when BCECF is H^+-free (reached at pH 9.0) and H^+-bound (reached at pH 5.0), respectively. The fluorescence ratio of S_b/S_a was determined as 0.45 ± 0.10 (total of n=8 fibres; mean ± SE). F_a and F_b are the fluorescence ratios at H^+-bound and H^+-free states, respectively, and were determined as 2.56 ± 0.22 for F_a and 8.63 ± 0.35 for F_b (total of n=8 fibres; mean ± SE).

When pH_i was measured during the contractile protocols, a modified Tydore´s solution was applied where 20 mM NaCl was substituted with NaLactate (101 mM NaCl, 5mM KCl, 1.8 mM $CaCl_2$, 0.5 mM $MgCl_2$, 0.4 mM NaH_2PO_4, 24 mM $NaHCO_3$, 5.5 mM glucose, 0.1 mM EGTA, 0.2% FBS and 20 mM NaLactate). This solution was applied in order to produce contractile-induced changes in intracellular pH in single mouse fibres (Westerblad & Allen, 1992).

Statistics

The experimental results are presented as mean ± standard deviation (SD). For comparison between two groups, paired Student's *t*-test were used and effect size was calculated using Cohen's d. For multiple comparisons, a one-way ANOVA followed by the Tukey test or a two-way ANOVA followed by Bonferroni test was used, as indicated. All the analyses were conducted using GraphPad Prism® version 4.00 for Windows (San Diego, California, USA). Statistical significance was accepted when $P<0.05$.

RESULTS

Influence of P_{O_2} and $NaNO_2$ administration on single fibre fatigue development

To assess the influence of $NaNO_2$ incubation on fatigue development and the potential P_{O_2}-dependence of this effect, single muscle fibres were exposed to either a supra-physiological or a near-physiological P_{O_2} [i.e., with 20% O_2 (~150 Torr) or 2% O_2 (~15.6Torr), respectively] in the absence of any injection or loading with fluorescent probes. At 20% O_2, time to task failure following $NaNO_2$ administration was 34 ± 19% shorter compared to standard Tyrode's solution (control: 257 ± 94 vs. $NaNO_2$: 159 ± 46 s; d=1.63, $P<0.05$, Fig. 2A, n=4 fibres). There were no differences in initial isometric force between the control and $NaNO_2$ fatigue runs at 20% O_2 (control: 413 ± 63 vs. $NaNO_2$: 410 ± 69 kPa; $P>0.05$). However, when fibres were superfused with 2% O_2, which was the smallest extracellular P_{O_2} that did not lower time to task failure compared to 20% O_2 (data not shown), $NaNO_2$ treatment increased time to task failure by 19 ± 18% (control: 538 ± 286 vs. $NaNO_2$: 607 ± 304 s, d=1.83, $P<0.05$, Fig. 2B, n=4 fibres). There was also no difference in initial isometric force between the control and $NaNO_2$ fatigue runs at 2% O_2 (control: 495 ± 111 vs. $NaNO_2$: 477 ± 98 kPa; $P>0.05$). There was no difference in time to task failure between the two fatigue runs at 2% O_2 when $NaNO_2$ was absent prior to and during the second fatigue-inducing contraction protocols (first fatigue run: 330 ± 131 vs. second fatigue run: 288 ± 143 s; $P>0.05$, n=4 fibres). When single muscle fibres were microinjected with FURA-2 to measure $[Ca^{2+}]_c$ responses during and between contractions, $NaNO_2$ treatment at near-physiological P_{O_2} did not increase time to task failure compared to the control condition (control: 142 ± 33 vs. $NaNO_2$: 165 ± 73 s, d=0.51, $P>0.05$, n=5 fibres). However, in fibres loaded with BCECF and perfused with a modified Tyrode's solution (i.e., with 20 mM NaLactate) to measure pH_i, time to task failure was increased with $NaNO_2$ administration (control: 291 ± 52 vs. $NaNO_2$: 379 ± 82 s; 31 ± 18% increase; d=1.62, $P<0.05$; n=5 fibres). When the fibres from all experiments at near-physiological P_{O_2} were pooled, time to task failure was enhanced by 21 ± 22% with $NaNO_2$ treatment compared to preceding control condition (control: 308 ± 217 vs. $NaNO_2$: 368 ± 242 s; d=1.14, $P<0.01$, Fig. 2C, n=14 fibres).

Influence of $NaNO_2$ on force and intracellular Ca^{2+} responses during single non-fatiguing contractions

During the single contraction non-fatiguing FF curves, maximal tetanic force was not different (P>0.05), but sub-maximal force during 20-50 Hz contractions was lowered in the $NaNO_2$ condition compared to the control condition (P<0.01, n=5 fibres; Fig 3A). For example, evoked force at 30 Hz was 42 ± 20% lower in the $NaNO_2$ condition (P<0.01). Peak $[Ca^{2+}]_c$ was lowered in the $NaNO_2$ condition at sub-maximal (e.g., by 21 ± 11% at 30 Hz, P<0.01) and maximal (e.g., by 22 ± 15% at 150 Hz, P<0.05) force development, as well as during 120 Hz contractions evoked in the presence of 10 mM caffeine (by 32 ± 21%), compared to the control condition (P<0.05). In fibres that were superfused with 2% O_2 but not treated with $NaNO_2$, maximal and submaximal forces were not different between the first and the second FF curves (data not shown, n=4, P>0.05). When isometric force development (shown in Fig 3A) was plotted against $[Ca^{2+}]_c$ (shown in Fig. 3B) across the FF curve, there were no differences between the control and $NaNO_2$ conditions (Fig. 3C). Indeed, the midpoints of the force-$[Ca^{2+}]_c$ curves were not different between the control and $NaNO_2$ conditions (e.g., $Ca^{2+}{}_{50}$ was 474 ± 154 nM vs. 472 ± 122 nM for control and $NaNO_2$, respectively, P>0.05, n=5 fibres).

Influence of $NaNO_2$ on intracellular Ca^{2+} responses during repeated fatigue-inducing contractions

There was no difference in peak $[Ca^{2+}]_c$ achieved during the evoked contractions between the control and $NaNO_2$ conditions throughout the fatigue-inducing contraction protocols (P>0.05, Fig. 4A). However, after 100 s of the fatigue-inducing contraction protocol, basal $[Ca^{2+}]_c$ following the evoked contractions was lower in the $NaNO_2$ condition (P<0.05). Moreover, basal $[Ca^{2+}]_c$ at the point of task failure was also lower in the $NaNO_2$ condition (109 ± 20 nM) compared to the control condition (136 ± 28 nM, d=1.33, P<0.05, Fig. 4B). The midpoint of the force-$[Ca^{2+}]_c$ curves ($Ca^{2+}{}_{50}$), an index for predict the myofilament Ca^{2+} sensitivity, was determined during the fatigue-inducing contractions and compared with the data obtained in the FF curves. While the $Ca^{2+}{}_{50}$ increased during the fatigue-inducing contraction protocol compared to the value obtained from the FF curve in the control condition (from 474 ± 154 nM to 601 ± 141 nM, P<0.05), the $Ca^{2+}{}_{50}$ was not different between the fatigue-inducing contraction protocol and the FF curve in the $NaNO_2$ condition (from 472 ± 122 nM to 566 ± 95 nM, P>0.05, Fig. 4C).

Influence of $NaNO_2$ on sarcoplasmic reticulum Ca^{2+} pumping during fatiguing contractions

There were no differences between the control and $NaNO_2$ conditions in the plot of $[Ca^{2+}]_c$ decay rate for each $[Ca^{2+}]_c$ following the first contraction of the repeated fatigue-inducing contraction protocol (Fig. 5A). Similarly, the rate of SR Ca^{2+} pumping following the first contraction was not different between the control (3323 ± 2209 $\mu M^{-3} \cdot s^{-1}$) and $NaNO_2$ (3069 ± 2276 $\mu M^{-3} \cdot s^{-1}$) conditions (P>0.05, Fig. 4D). During the fatigue-inducing contraction protocol, the rate of SR Ca^{2+} pumping was slower after 80 s (534 ± 543 $\mu M^{-3} \cdot s^{-1}$) compared to the first contraction (P<0.05) and slower at the time of task failure (200 ± 217 $\mu M^{-3} \cdot s^{-1}$) compared to both the first contraction and after 80 s of the fatigue-inducing contraction protocol in the control condition (P<0.05). Likewise, the rate of SR Ca^{2+} pumping was progressively slowed from the first contraction, after 80 s (955 ± 854 $\mu M^{-3} \cdot s^{-1}$) and at the time of task failure (486 ± 380 $\mu M^{-3} \cdot s^{-1}$) during the fatigue-inducing contraction protocol in the $NaNO_2$ condition (P<0.05). After 80 s of contractions (Fig. 5B) and at the time of task failure (Fig. 5C), the plots of $[Ca^{2+}]_c$ decay rate for each $[Ca^{2+}]_c$ were left-shifted in the $NaNO_2$ condition compared to the control condition. Moreover, compared to the control condition, the rate of SR Ca^{2+} pumping was 110 ± 78% (d=0.63) and 212 ± 105% (d=0.97) higher with $NaNO_2$ treatment after 80 s of contractions (Fig. 5E) and at the time of task failure (Fig. 5F), respectively, during the fatigue-inducing contraction protocol (P<0.05).

Intracellular pH changes during fatiguing contractions

Compared to the resting values, pH_i at task failure was lower in both the control (Pre: 7.46 ± 0.23 vs. Post: 7.34 ± 0.22) and $NaNO_2$ (Pre: 7.46 ± 0.24 vs. Post: 7.25 ± 0.21) conditions (P<0.0001, n=5 fibres, Fig. 6). There were no differences in pH_i between the control and $NaNO_2$ conditions over the first 300 s of the fatigue-inducing contraction protocol (P>0.05). However, the change in pH_i from the start to the end of the fatigue-inducing contraction protocol was greater in the $NaNO_2$ condition (-0.20 ± 0.04) compared to the control condition (-0.12 ± 0.05, P<0.05).

DISCUSSION

The important original findings from this study were that $NaNO_2$ exposure delayed fatigue development in single mammalian skeletal muscle fibres at a near-physiological P_{O_2}, but expedited fatigue development at a supra-physiological P_{O_2}, during a repeated tetanic contraction protocol. Moreover, when single skeletal muscle fibres were incubated with NaLactate to replicate the contraction-induced decline in pH_i that is manifest *in vivo*, the blunting of fatigue development with $NaNO_2$ compared to the control condition at a physiological P_{O_2} was greater than the same comparison without NaLactate coincubation. The delayed fatigue development with $NaNO_2$ administration did not impact peak $[Ca^{2+}]_c$ during the fatiguing contraction protocol but blunted the progressive decline in SR Ca^{2+} pumping rate and the associated increase in basal $[Ca^{2+}]_c$ in the recovery period between contractions. Incubation with $NaNO_2$ also alleviated the decline in myofilament Ca^{2+} sensitivity during the fatiguing contraction protocol. There was no difference in pH_i between the $NaNO_2$ and control conditions over the first 300 s of the fatigue-inducing contraction protocol, but pH_i was lower at task failure in the $NaNO_2$ condition compared to the control condition. These results suggest that, at a P_{O_2} comparable to that observed in human skeletal muscle during fatigue-inducing contractions (Richardson *et al*., 1995), and in the absence of any alterations in perfusion, NO_2^- treatment can delay the development of fatigue in single skeletal muscle fibres by improving SR Ca^{2+} pumping, maintaining Ca^{2+} sensitivity, and permitting the attainment of a lower pH_i. These findings extend our understanding of the mechanisms by which increased muscle NO_2^- exposure, as occurs following dietary NO_3^- supplementation (Gillard *et al*., 2018; Wylie *et al*., in press), can blunt skeletal muscle fatigue and suggest that the potential for NO_2^- administration to attenuate fatigue development is P_{O_2}- and pH-dependent.

Influence of $NaNO_2$ administration on time to task failure at a near-physiological P_{O_2}

Incubation with $NaNO_2$ at a near-physiological P_{O_2} increased time to task failure by 19% compared to the control condition with no fluorophore loading. Although $NaNO_2$ administration at a near-physiological P_{O_2} did not increase time to task failure in fibres microinjected with FURA-2 to assess $[Ca^{2+}]_c$ dynamics, when these data were combined with data from fibres with no fluorophore loading, time to task failure was extended by 15%. The greatest increase (31%

compared to the respective control condition) in time to task failure with $NaNO_2$ incubation in the current study was observed when skeletal muscle fibres were co-incubated with a near-physiological P_{O_2} and NaLactate to facilitate a decline in pH_i (Westerblad & Allen, 1992) and thus better reflect the pH_i dynamics in human skeletal muscle *in vivo* (Vanhatalo *et al*., 2011). The mean improvement in time to task failure with $NaNO_2$ incubation compared to the respective control conditions in the experiments completed with (FURA-2 and BCECF-AM) and without fluorophores was 21% at a near-physiological P_{O_2} in the current study.

It has been reported that intracellular P_{O_2} in both rodent and human skeletal muscle fibres drops from ~30 Torr at rest to ~3-4 Torr during intense exercise (Hirai *et al*., 2018; Richardson *et al.*, 1995). The extracellular P_{O_2} was set at ~15 Torr (2% O_2) in the current study as preliminary experiments revealed this to be the smallest extracellular P_{O_2} that did not lower time to fatigue in single skeletal muscle fibres compared to experiments conducted at 20% O_2, which suggest that at 15 Torr fibres were not under hypoxic conditions during contractions. Furthermore, the extracellular P_{O_2} used in the present work closely reflects the P_{O_2} in the interstitial space between the capillaries and muscle fibres (Hirai *et al*., 2018), and was intended to replicate the intracellular P_{O_2} during contractions in humans *in vivo* (Richardson *et al*., 1995). Although the control fatigue-inducing protocol always preceded the $NaNO_2$ fatigue-inducing protocol, there was no difference in evoked isometric force in the first tetanic contraction of the control and $NaNO_2$ fatigue-inducing protocols, and there was no difference in time to task failure between two fatigue-inducing protocols at 2% O_2 without $NaNO_2$ administration. Therefore, our results suggest that, at a near physiological P_{O_2}, the blunted rate of fatigue development in the second fatigue-inducing protocol completed with $NaNO_2$ administration was not confounded by differences in initial force production or fatigue development between the first and second fatigue-inducing contraction protocols.

Influence of $NaNO_2$ administration on time to fatigue at a supra-physiological P_{O_2}

In contrast to the delayed rate of fatigue development with $NaNO_2$ administration at a near physiological P_{O_2}, fatigue development was expedited when $NaNO_2$ was administered at a supra-physiological P_{O_2} of 20% O_2 (~150 Torr) in the present study. It has been reported that sarcomere shortening and $[Ca^{2+}]_c$ are greater in collagenase-digested single FDB muscle fibres

excised from wild-type mice and stimulated by single twitches at 1% O_2 compared to 20% O_2, and that these effects are abolished in fibres excised from nNOS knock-out mice (Eu *et al*., 2003). These findings suggest that, at least in the unfatigued state, SR Ca^{2+} handling and skeletal muscle contractility are improved by NO production at a physiological P_{O_2} compared to a supra-physiological P_{O_2}. It has been suggested that the one-electron reduction of NO_2^- to NO is inversely related to P_{O_2} and that the oxidation of NO_2^- and NO to NO_3^- is increased at a higher P_{O_2} (Lundberg & Weitzberg, 2009, 2010). The greater production of superoxide in hyperoxia (Clanton, 2007) will also act to scavenge NO generated from NO_2^- reduction (Sjöberg & Singer, 2013) leading to the formation of the potent oxidising agent, peroxynitrite (Radi, 2013). This potential for increased peroxynitrite synthesis with NO_2^- administration at a supra-physiological P_{O_2} might have contributed to the earlier attainment of task failure compared to the control condition (Dutka *et al*., 2012; Supinski *et al*., 1999). There is also evidence that hydrogen peroxide, which is generated through the dismutation of superoxide, can oxidise NO_2^- to NO_3^- through the enzyme, catalase (Heppel & Porterfield, 1949). Therefore, the P_{O_2}-dependent effects of NO_2^- on fatigue development might be linked to the proportion of NO_2^- that is reduced to NO and its interaction with reactive oxygen species. Collectively, our results suggest that the effect of $NaNO_2$ administration on fatigue development in single skeletal muscle fibres is P_{O_2}- and pH-dependent with the greatest positive effect manifest when P_{O_2} and pH_i dynamics most closely resemble those that are exhibited in human skeletal muscle *in vivo*.

Influence of $NaNO_2$ administration on skeletal muscle Ca^{2+} handling

In addition to measuring fatigue development, $[Ca^{2+}]_c$ transients were assessed during a series of single non-fatiguing contractions and during subsequent repeated fatigue-inducing tetanic contractions at a near physiological P_{O_2} in the absence and presence of $NaNO_2$. There were no differences in isometric force during a series of single contractions evoked prior to and 60 min following the completion of a repeated contraction fatigue-inducing protocol suggesting that 60 min of recovery was sufficient to restore isometric force to baseline. Accordingly, any effect of NO_2^- on contractility during the second series of single non-fatiguing contractions would not be expected to be confounded by the preceding fatigue-inducing contraction protocol. During the series of single non-fatiguing contractions completed 60 min after the end of the first bout of fatiguing contractions and with $NaNO_2^-$ incubation, isometric force during single submaximal

(20-50 Hz) contractions was depressed compared to the initial control condition, but not at near-maximal or maximal (>50 Hz) contractions. $[Ca^{2+}]_c$ was lower with NO_2^- treatment during single 30-150 Hz contractions and during a single 120 Hz contraction in the presence of 10 mM caffeine to evoke maximum SR Ca^{2+} release, but due to the sigmoidal nature of the force-Ca^{2+} relationship, the decreased in peak $[Ca^{2+}]_c$ at high pulse-frequencies with $NaNO_2$ did not alter the maximum force developed. Therefore, the suppression of isometric force development during sub-maximal contractions with NO_2^- exposure was a function of lower SR Ca^{2+} release with no change in Ca^{2+} sensitivity. In contrast, and despite administering the same NO_2^- dose as the current study, $[Ca^{2+}]_c$ was increased, and isometric force was attenuated in single mouse skeletal muscle fibres with NO_2^- treatment at 95% O_2 in a previous study by Andrade *et al*. (1998b). Since this reduction in myofibrillar Ca^{2+} sensitivity with NO_2^- treatment was also observed following the administration of different NO donors (Andrade *et al*., 1998b), these findings suggest that the effects of NO_2^- on SR Ca^{2+} handling are NO-mediated or that NO_2^- and NO impact SR Ca^{2+} handling through common signalling mechanisms. The disparate effect of NO_2^- on SR Ca^{2+} handling and isometric force in the current study and the study by Andrade *et al*. (1998b) is likely a function of the inter-study difference in the experimental P_{O_2} (Eu *et al*., 2003) and its influence on the crosstalk between redox and nitroso signalling (Spencer & Posterino, 2009). While it is unclear why NO_2^- administration suppressed isometric force production and peak $[Ca^{2+}]_c$ during 20-50 Hz submaximal contractions, and did not change isometric force production during maximal/near-maximal contractions at 100 Hz, these observations are in line with previous findings that NO donors are more likely to impair force production during unfused tetanus compared to fused tetanus (Maréchal and Gailly, 1999; Murrant *et al*., 1997).

During the fatigue-inducing repeated tetanic contraction protocol, peak $[Ca^{2+}]_c$ during contractions declined, basal $[Ca^{2+}]_c$ following contractions increased and myofibrillar Ca^{2+} sensitivity was lowered as the fatigue protocol progressed. These perturbations to SR Ca^{2+} handling are consistent with previous reports and are important contributors to the development of skeletal muscle fatigue (Allen *et al*., 2008; Westerblad & Allen, 1994). There was no difference in peak $[Ca^{2+}]_c$ during contractions between the $NaNO_2$ and control conditions throughout the fatigue run. However, after 80 s of the fatigue run, the slowing in SR Ca^{2+} pumping and the resultant increase in basal $[Ca^{2+}]_c$ following contractions were attenuated with

NO_2^- treatment. Therefore, the blunted fatigue development in the NO_2^- trial compared to the control trial appears to be linked to a better maintenance of SR Ca^{2+} pumping. The pumping of Ca^{2+} by the SR is an active process that is coupled to the function (Ca^{2+} affinity and the coupling between ATP hydrolysis and Ca^{2+} transport) of the SR Ca^{2+}-ATPase (SERCA). SERCA function is regulated by the phosphorylation status of two proteins with similar structures, phospholamban, which is mostly expressed in cardiac myocytes and in slow-twitch muscle fibres, and sarcolipin, which is mostly expressed in skeletal muscle fibres (Pant *et al*., 2016). Specifically, phosphorylated phospholamban and sarcolipin can improve SERCA function, whereas dephosphorylated phospholamban and sarcolipin can compromise SERCA function (Tupling, 2009). It has been reported that NO_2^- administration can increase the amount of phosphorylated phospholamban in striated muscle through nitrite reductase dependent NO production (Huang *et al*., 2013). Therefore, it is possible phosphorylation of phospholamban and/or sarcolipin might have contributed to the improved maintenance of SR Ca^{2+} pumping during the fatigue-inducing contraction protocol completed with $NaNO_2$ treatment at a low P_{O_2} compared to the control trial in the current study. Moreover, since the rate of SR Ca^{2+} pumping is inversely related to basal $[Ca^{2+}]_c$ accumulation during repetitive contractions (Nogueira *et al.*, 2013, 2018), the lower basal $[Ca^{2+}]_c$ accumulation during the fatigue-inducing contraction protocol would also likely have contributed to the better maintenance of SR Ca^{2+} pumping during the NO_2^- trial. Lowering the energy cost of actomyosin ATPase, through inhibiting cross-bridge cycling, has also been reported to abate the progressive slowing in SR Ca^{2+} pumping rate during fatiguing contractions (Nogueira *et al.*, 2013). It has been reported that increasing NO_2^- via short-term dietary NO_3^- supplementation can lower the high-energy phosphate cost of sub-maximal (Bailey *et al*., 2010) and maximal (Fulford *et al*., 2013) skeletal muscle force production, which is compatible with findings from single intact skeletal muscle fibres that the energy cost of skeletal muscle contraction impacts SR Ca^{2+} pumping rate during fatiguing contractions (Nogueira *et al.*, 2013).

Compared to the single non-fatiguing contractions completed during the construction of the force-frequency curve, myofilament Ca^{2+} sensitivity declined across the fatigue-inducing contraction protocol in the control trial, but not the $NaNO_2$ trial. Therefore, improved preservation of myofilament Ca^{2+} sensitivity might have contributed to the slower rate of fatigue

development in the $NaNO_2$ trial. It has been reported that treatment with NO donors can S-nitrosylate cysteine residues in the myosin heavy chain leading to slowed cross-bridge cycling (Nogueira *et al*., 2009), but increased force per power stroke (Evangelista *et al*., 2010). Since NO_2^- administration has also been reported to promote S-nitrosylation in striated muscle (Kovács *et al*., 2015), the improved maintenance of Ca^{2+} sensitivity with $NaNO_2$ administration in the current study might therefore be a function of direct NO_2^- action on the myofilaments. Alternatively, NO_2^- administration might have improved myofilament Ca^{2+} sensitivity indirectly through attenuating ROS production (Yang *et al*., 2015), or thwarting ROS-mediated oxidation of the myofilaments (Moonpanar & Allen, 2006).

Influence of $NaNO_2$ administration on skeletal muscle pH

Since a decline in muscle pH has been reported to compromise myofilament Ca^{2+} sensitivity (Fabiato & Fabiato, 1978) and SERCA function (Wolosker *et al*., 1997), and since NO has been reported to inhibit glycolysis via S-nitrosylation of glyceraldehyde-3-phosphate dehydrogenase (Mohr *et al*., 1996), pH_i was assessed to provide insight into the potential mechanisms for improved Ca^{2+} handling in the $NaNO_2$ trial. Since pH_i was not different between the $NaNO_2$ and control trials over the first 300 s of the fatigue run, the results presented in this study suggest that the improved maintenance of myofilament Ca^{2+} sensitivity and SR Ca^{2+} pumping rate in the $NaNO_2$ trial extended time to task failure and permitted the attainment of a lower pH_i at task failure compared to the control condition.

Limitations and areas for further research

We combined the time to task failure data from FURA-2 injected fibres and non-injected fibres as time to task failure was not significantly different with $NaNO_2$ compared to the control condition in FURA-2 microinjected fibres. Therefore, it should be acknowledged that the experiments in FURA-2 injected fibres to assess the effects of $NaNO_2$ administration on Ca^{2+} handling and fatigue at a near-physiological P_{O_2} in the current study were underpowered. When the data from FURA-2 injected fibres and non-injected fibres were combined, time to task failure was significantly extended in the $NaNO_2$ condition, consistent with the experiments where $NaNO_2$ was co-incubated with NaLactate to facilitate a decline in pH_i. Therefore, this approach does not undermine the conclusion that acute $NaNO_2$ administration can delay fatigue

development at a near-physiological P_{O_2} and we have based our conclusions on the effect of $NaNO_2$ administration on fatigue development when all fibres are pooled. Since acute NO_2^- exposure lowered $[Ca^{2+}]_c$ and force during 20-50 Hz isometric contractions in the current study, but elevating plasma $[NO_2^-]$ via chronic NO_3^- supplementation increased these variables in the same experimental model (Hernández *et al*., 2012), we cannot exclude the possibility that skeletal muscle contractility, fatigue, and Ca^{2+} handling might be enhanced to a greater extent after chronic NO_3^- supplementation. It should be noted that since mammalian plasma nitrite is significantly lower (i.e., at high nanomolar range) after NO_3^- ingestion (e.g., Wylie et al., 2013) compared to the 100 µM $NaNO_2^-$ that was used to perfuse the skeletal muscle fibres in the present investigation, the dose of NO_2^- administered in the current study was supraphysiological. Furthermore, since human skeletal muscles do not manifest the same changes in Ca^{2+}-handling proteins following a 7-day NO_3^- supplementation (Whitfield *et al*., 2017) previously detected in rodent skeletal muscle (Hernández *et al*., 2012), the extent to which our findings translate to humans is unclear and in need of further research.

While fatigue development was attenuated concomitant with improved Ca^{2+} handling following $NaNO_2$ administration at a physiological P_{O_2}, Ca^{2+} handling was not assessed during the supraphysiological P_{O_2} experiments in the current study. Therefore, the mechanisms for the more rapid fatigue development with $NaNO_2$ administration at a supraphysiological P_{O_2} remains to be determined. Moreover, although the contraction-induced pH_i changes observed in the present study were qualitatively similar to the contraction-induced pH_i changes in human skeletal muscle *in vivo*, it should be acknowledged that the solution that all fibres were superfused with was bubbled with 5% CO_2 for an extracellular final pH ~7.4. Therefore, pH_i was higher in the present study compared to human skeletal muscle completing fatiguing contractions *in vivo*. It is also acknowledged that a limitation of our study is the lack of measurement of NO/ROS markers. Since the NO fluorescent probes, DAF-FM and DAF-2, do not detect NO at low oxygen tensions (Namin et al, 2013), these probes could not be employed to assess myofiber NO production from NO_2^- reduction in our study. Further research is required to assess the effects of increased skeletal muscle NO_2^- exposure on NO and ROS signalling in skeletal muscle.

Translational Perspective

Over the past decade there has been significant interest in supplementing the diet with NO_3^- to enhance exercise economy and performance (Jones, 2014), but the underpinning mechanisms for these effects were unclear. The present study indicates that $NaNO_2$ administration can delay fatigue development, improve the maintenance of myofilament Ca^{2+} sensitivity and attenuate the fatigue-induced slowing in SR Ca^{2+} reuptake during repeated tetanic contractions in *ex vivo* skeletal muscle fibres at a near-physiological P_{O_2} of 2% O_2. These findings using a single skeletal muscle fibre model also demonstrate that increased NO_2^- exposure can blunt skeletal muscle fatigue development independent of any alterations in skeletal muscle perfusion by improving skeletal muscle Ca^{2+} handling. Therefore, our findings offer novel insights into some of the mechanisms that might underpin the ergogenic effects of increased skeletal muscle NO_2^- exposure, which might have implications for improving understanding of how dietary NO_3^- supplementation is ergogenic in humans during high-intensity endurance exercise.

In addition to evoking positive effects in skeletal muscle, NO_3^- supplementation or administration of NO donors can improve Ca^{2+} handling and contractile function in cardiomyocytes (Pironti *et al*., 2016; Tocchetti *et al*., 2007). There is also evidence to suggest that NO_3^- supplementation can improve skeletal muscle (Coggan *et al*., 2015b) and cardiac (Zamani *et al*., 2015) function, and exercise capacity (Coggan *et al*., 2018; Zamani *et al*., 2015) in heart failure patients. Therefore, increased NO_2^- exposure following NO_3^- supplementation might have important therapeutic application in patients with diseases of the cardiovascular system.

In conclusion, acute treatment with $NaNO_2$ delayed time to task failure in intact skeletal muscle fibres at a physiological P_{O_2} during a repeated tetanic isometric contraction protocol. The greatest attenuation of fatigue development was observed when NaLactate was co-administered with $NaNO_2$ at 2% O_2 to elicit similar pH_i response dynamics to those manifest *in vivo*. Conversely, task failure was attained earlier following $NaNO_2$ administration when assessed at a supra-physiological P_{O_2} equivalent to 20% O_2. The delay in fatigue development following $NaNO_2$ administration at 2% O_2 was accompanied by improved maintenance of myofilament Ca^{2+} sensitivity, increased SR Ca^{2+} pumping and a lower basal $[Ca^{2+}]_c$ in the recovery period between contractions, and a greater decline of pH_i. Therefore, $NaNO_2$ administration can delay

fatigue development in intact, *ex vivo* skeletal muscle fibres at a near-physiological P_{O_2}, with this effect linked to improved myocyte Ca^{2+} handling. These results provide new insight into the mechanisms by which increased NO_2^- exposure can mitigate skeletal muscle fatigue development and the ergogenic potential of dietary NO_3^- ingestion.

REFERENCES

Allen DG, Lamb GD & Westerblad H. (2008). Skeletal muscle fatigue: cellular mechanisms. *Physiol Rev* **88,** 287-332.

Andrade FH, Reid MB, Allen DG & Westerblad H. (1998a). Effect of hydrogen peroxide and dithiothreitol on contractile function of single skeletal muscle fibres from the mouse. *J Physiol* **509,** 565-575.

Andrade FH, Reid MB, Allen DG & Westerblad H. (1998b). Effect of nitric oxide on single skeletal muscle fibres from the mouse. *J Physiol* **509,** 577-586.

Bailey SJ, Fulford J, Vanhatalo A, Winyard PG, Blackwell JR, DiMenna FJ, Wilkerson DP, Benjamin N, Jones AM. (2010). Dietary nitrate supplementation enhances muscle contractile efficiency during knee-extensor exercise in humans. *J Appl Physiol* **109**, 135-48.

Bailey SJ, Winyard P, Vanhatalo A, Blackwell JR, Dimenna FJ, Wilkerson DP, Tarr J, Benjamin N, Jones AM (2009). Dietary nitrate supplementation reduces the O_2 cost of low-intensity exercise and enhances tolerance to high-intensity exercise in humans. *J Appl Physiol* **107**, 1144-1155.

Bakker AJ, Head SI, Williams DA & Stephenson DG. (1993). Ca^{2+} levels in myotubes grown from the skeletal muscle of dystrophic (mdx) and normal mice. *J Physiol* **460,** 1-13.

Barclay CJ. (2015). Energetics of contraction. *Compr Physiol* **5**, 961-995.

Castello PR, David PS, McClure T, Crook Z, Poyton RO. (2006). Mitochondrial cytochrome oxidase produces nitric oxide under hypoxic conditions: implications for oxygen sensing and hypoxic signaling in eukaryotes. *Cell Metab*. **3**,277-87.

Clanton TL. (2007). Hypoxia-induced reactive oxygen species formation in skeletal muscle. J Appl Physiol. 102, 2379-2388.

Clanton TL. (2019). Managing the power grid: how myoglobin can regulate PO_2 and energy distribution in skeletal muscle. *J Appl Physiol*. **126**, 787-790.

Coggan AR, Broadstreet SR, Mahmood K, Mikhalkova D, Madigan M, Bole I, Park S, Leibowitz JL, Kadkhodayan A, Thomas DP, Thies D, Peterson LR. (2018). Dietary Nitrate Increases VO_2peak and Performance but Does Not Alter Ventilation or Efficiency in Patients With Heart Failure With Reduced Ejection Fraction. *J Card Fail* **24**, 65-73.

Coggan AR, Leibowitz JL, Kadkhodayan A, Thomas DP, Ramamurthy S, Spearie CA, Waller S, Farmer M, Peterson LR. (2015a). Effect of acute dietary nitrate intake on maximal knee extensor speed and power in healthy men and women. *Nitric Oxide* **48**, 16-21.

Coggan AR, Leibowitz JL, Spearie CA, Kadkhodayan A, Thomas DP, Ramamurthy S, Mahmood K, Park S, Waller S, Farmer M, Peterson LR. (2015b). Acute Dietary Nitrate Intake Improves Muscle Contractile Function in Patients With Heart Failure: A Double-Blind, Placebo-Controlled, Randomized Trial. *Circ Heart Fail* **8**, 914-920.

Drummond GB. (2009). Reporting ethical matters in the Journal of Physiology: standards and advice. *J Physiol* **587,** 713-719.

Dutka TL, Verburg E, Larkins N, Hortemo KH, Lunde PK, Sejersted OM, Lamb GD. (2012). ROS-mediated decline in maximum Ca2+-activated force in rat skeletal muscle fibers following in vitro and in vivo stimulation. *PLoS One*. 7(5):e35226.

Eu JP, Hare JM, Hess DT, Skaf M, Sun J, Cardenas-Navina I, Sun QA, Dewhirst M, Meissner G, Stamler JS. (2003). Concerted regulation of skeletal muscle contractility by oxygen tension and endogenous nitric oxide. *Proc Natl Acad Sci U S A* **100**, 15229-15234.

Evangelista AM, Rao VS, Filo AR, Marozkina NV, Doctor A, Jones DR, Gaston B, Guilford WH. (2010). Direct regulation of striated muscle myosins by nitric oxide and endogenous nitrosothiols. *PLoS One* **5(6)**:e11209.

Fabiato A, Fabiato F. (1978). Effects of pH on the myofilaments and the sarcoplasmic reticulum of skinned cells from cardiace and skeletal muscles. *J Physiol* **276**, 233-255.

Ferguson SK, Hirai DM, Copp SW, Holdsworth CT, Allen JD, Jones AM, Musch TI, Poole DC. (2013). Impact of dietary nitrate supplementation via beetroot juice on exercising muscle vascular control in rats. *J Physiol* **591**, 547-57.

Ferguson SK, Holdsworth CT, Wright JL, Fees AJ, Allen JD, Jones AM, Musch TI, Poole DC. (2015). Microvascular oxygen pressures in muscles comprised of different fiber types: Impact of dietary nitrate supplementation. *Nitric Oxide* **48**, 38-43.

Fulford J, Winyard PG, Vanhatalo A, Bailey SJ, Blackwell JR, Jones AM. (2013). Influence of dietary nitrate supplementation on human skeletal muscle metabolism and force production during maximum voluntary contractions. *Pflugers Archive* **465**, 517-528.

Gandra PG, Shiah AA, Nogueira L, Hogan MC. (2018). A mitochondrial-targeted antioxidant improves myofilament Ca^{2+} sensitivity during prolonged low frequency force depression at low PO2. *J Physiol*. **596**, 1079-1089.

Gilliard CN, Lam JK, Cassel KS, Park JW, Schechter AN, Piknova B. (2018). Effect of dietary nitrate levels on nitrate fluxes in rat skeletal muscle and liver. *Nitric Oxide*. **75**, 1-7.

Haider G, Folland JP. (2014). Nitrate supplementation enhances the contractile properties of human skeletal muscle. *Med Sci Sports Exerc* **46**, 2234-2243.

Heppel LA, Porterfield VT. (1949). Metabolism of inorganic nitrite and nitrate esters; the coupled oxidation of nitrite by peroxide-forming systems and catalase. *J Biol Chem* **178**, 549-556.

Hernández A, Schiffer TA, Ivarsson N, Cheng AJ, Bruton JD, Lundberg JO, Weitzberg E, Westerblad H. (2012). Dietary nitrate increases tetanic $[Ca^{2+}]i$ and contractile force in mouse fast-twitch muscle. *J Physiol* **590**, 3575-3583.

Hirai DM, Craig JC, Colburn TD, Eshima H, Kano Y, Sexton WL, Musch TI, Poole DC. (2018). Skeletal muscle microvascular and interstitial PO2 from rest to contractions. *J Physiol*. **596**: 869-883.

Huang Y, He Q, Zhan L, Yang M. (2013). Sarcoplasmic phospholamban protein is involved in the mechanisms of postresuscitation myocardial dysfunction and the cardioprotective effect of nitrite during resuscitation. *PLoS One*. 8(12):e82552.

Ignarro LJ, Buga GM, Wood KS, Byrns RE, Chaudhuri G. (1987). Endothelium-derived relaxing factor produced and released from artery and vein is nitric oxide. *Proc Natl Acad Sci U S A* **84**, 9265-9269.

Ivarsson N, Schiffer TA, Hernández A, Lanner JT, Weitzberg E, Lundberg JO, Westerblad H. (2017). Dietary nitrate markedly improves voluntary running in mice. *Physiol Behav*. **168**, 55-61.

Jones AM. (2014). Dietary nitrate supplementation and exercise performance. *Sports Med* **44**, 35-45.

Kelly J, Vanhatalo A, Bailey SJ, Wylie LJ, Tucker C, List S, Winyard PG, Jones AM. (2014). Dietary nitrate supplementation: effects on plasma nitrite and pulmonary O_2 uptake dynamics during exercise in hypoxia and normoxia. *Am J Physiol Regul Integr Comp Physiol* **307**, 920-930.

Klein MG, Kovacs L, Simon BJ & Schneider MF. (1991). Decline of myoplasmic Ca2+, recovery of calcium release and sarcoplasmic Ca^{2+} pump properties in frog skeletal muscle. *J Physiol* **441,** 639-671.

Kovács M, Kiss A, Gönczi M, Miskolczi G, Seprényi G, Kaszaki J, Kohr MJ, Murphy E, Végh Á. (2015). Effect of sodium nitrite on ischaemia and reperfusion-induced arrhythmias in anaesthetized dogs: is protein S-nitrosylation involved? *PLoS One* **10(4)**:e0122243.

Larsen FJ, Schiffer TA, Borniquel S, Sahlin K, Ekblom B, Lundberg JO, Weitzberg E. (2011). Dietary inorganic nitrate improves mitochondrial efficiency in humans. *Cell Metab* **13**, 149-59.

Larsen FJ, Weitzberg E, Lundberg JO, Ekblom B. (2007). Effects of dietary nitrate on oxygen cost during exercise. *Acta Physiol (Oxf)* **191**, 59-66.

Lundberg JO, Weitzberg E. (2010). NO-synthase independent NO generation in mammals. *Biochem Biophys Res Commun* **396**, 39-45.

Lundberg JO, Weitzberg E. (2009). NO generation from inorganic nitrate and nitrite: Role in physiology, nutrition and therapeutics. *Arch Pharm Res* **32**, 1119-1126.

McDonough P, Behnke BJ, Padilla DJ, Musch TI, Poole DC. (2005). Control of microvascular oxygen pressures in rat muscles comprised of different fibre types. *J Physiol* **563**, 903-913.

Maréchal G, Gailly P. (1999). Effects of nitric oxide on the contraction of skeletal muscle. *Cell Mol Life Sci*. **55**, 1088-1102.

Modin A, Björne H, Herulf M, Alving K, Weitzberg E, Lundberg JO. (2001). Nitrite-derived nitric oxide: a possible mediator of 'acidic-metabolic' vasodilation. *Acta Physiol Scand* **171**, 9-16.

Mohr S, Stamler JS, Brüne B. (1996). Posttranslational modification of glyceraldehyde-3-phosphate dehydrogenase by S-nitrosylation and subsequent NADH attachment. *J Biol Chem* **271**, 4209-4214.

Moncada S, Higgs EA. (1991). Endogenous nitric oxide: physiology, pathology and clinical relevance. *Eur J Clin Invest* **21**, 361-374.

Moopanar TR, Allen DG. (2006). The activity-induced reduction of myofibrillar Ca2+ sensitivity in mouse skeletal muscle is reversed by dithiothreitol. *J Physiol* **571**, 191-200.

Murad F, Mittal CK, Arnold WP, Katsuki S, Kimura H (1978). Guanylate cyclase: activation by azide, nitro compounds, nitric oxide, and hydroxyl radical and inhibition by hemoglobin and myoglobin. *Adv Cyclic Nucleotide Res* **9**, 145-158.

Murrant CL, Frisbee JC, Barclay JK. (1997). The effect of nitric oxide and endothelin on skeletal muscle contractility changes when stimulation is altered. *Can J Physiol Pharmacol*. **75**, 414-22.

Namin SM, Nofallah S, Joshi MS, Kavallieratos K, Tsoukias NM. (2013). Kinetic analysis of DAF-FM activation by NO: toward calibration of a NO-sensitive fluorescent dye. *Nitric Oxide* **28**, 39-46.

Nogueira L & Hogan MC. (2010). Phenol increases intracellular [Ca2+] during twitch contractions in intact Xenopus skeletal myofibers. *J Appl Physiol* **109,** 1384-1393.

Nogueira L, Figueiredo-Freitas C, Casimiro-Lopes G, Magdesian MH, Assreuy J, Sorenson MM. (2009). Myosin is reversibly inhibited by S-nitrosylation. *Biochem J*. **424**, 221-231.

Nogueira L, Shiah AA, Gandra PG & Hogan MC. (2013). Ca(2)(+)-pumping impairment during repetitive fatiguing contractions in single myofibers: role of cross-bridge cycling. *Am J Physiol Regul Integr Comp Physiol* **305,** 118-125.

Nogueira L, Trisko BM, Lima-Rosa FL, Jackson J, Lund-Palau H, Yamaguchi M, Breen EC. (2018). Cigarette smoke directly impairs skeletal muscle function through capillary regression and altered myofibre calcium kinetics in mice. *J Physiol*. **596**, 2901-2916.

Pant M, Bal NC, Periasamy M. (2016). Sarcolipin: A Key Thermogenic and Metabolic Regulator in Skeletal Muscle. *Trends Endocrinol Metab*. **27**, 881-892.

Porcelli S, Ramaglia M, Bellistri G, Pavei G, Pugliese L, Montorsi M, Rasica L, Marzorati M. (2015). Aerobic Fitness Affects the Exercise Performance Responses to Nitrate Supplementation. *Med Sci Sports Exerc* **47**, 1643-1651.

Radi R. (2013). Peroxynitrite, a stealthy biological oxidant. *J Biol Chem*. **288**, 26464-26472.

Richardson RS, Noyszewski EA, Kendrick KF, Leigh JS & Wagner PD. (1995). Myoglobin O_2 desaturation during exercise. Evidence of limited O2 transport. *J Clin Invest* **96,** 1916-1926.

Sjöberg F, Singer M. (2013). The medical use of oxygen: a time for critical reappraisal. *J Intern Med* **274**, 505-28.

Spencer T, Posterino GS. (2009). Sequential effects of GSNO and H_2O_2 on the Ca^{2+} sensitivity of the contractile apparatus of fast- and slow-twitch skeletal muscle fibers from the rat. *Am J Physiol Cell Physiol* **296**, 1015-1023.

Stamler JS, Meissner G. (2001). Physiology of nitric oxide in skeletal muscle. *Physiol Rev* **81**, 209-237.

Suhr F, Gehlert S, Grau M, Bloch W (2013). Skeletal muscle function during exercise-fine-tuning of diverse subsystems by nitric oxide. *Int J Mol Sci* **14**, 7109-7139.

Supinski G, Stofan D, Callahan LA, Nethery D, Nosek TM, DiMarco A. (1999). Peroxynitrite induces contractile dysfunction and lipid peroxidation in the diaphragm. J Appl Physiol. **87**, 783-791.

Tanaka Y, Poole DC, Kano Y. (2016). pH Homeostasis in Contracting and Recovering Skeletal Muscle: Integrated Function of the Microcirculation with the Interstitium and Intramyocyte Milieu. *Curr Top Med Chem* **16**, 2656-2563.

Tupling AR. (2009). The decay phase of Ca^{2+} transients in skeletal muscle: regulation and physiology. *Appl Physiol Nutr Metab 34*, 373-376.

Vanhatalo A, Fulford J, Bailey SJ, Blackwell JR, Winyard PG, Jones AM. (2011). Dietary nitrate reduces muscle metabolic perturbation and improves exercise tolerance in hypoxia. *J Physiol* **589**, 5517-5528.

Walsh B, Stary CM, Howlett RA, Kelley KM & Hogan MC. (2008). Glycolytic activation at the onset of contractions in isolated Xenopus laevis single myofibres. *Exp Physiol* **93,** 1076-1084.

Walsh B, Howlett RA, Stary CM, Kindig CA, Hogan MC. (2006). Measurement of activation energy and oxidative phosphorylation onset kinetics in isolated muscle fibers in the absence of cross-bridge cycling. Am J Physiol Regul Integr Comp Physiol. 290, 1707-1713.

Westerblad H & Allen DG. (1991). Changes of myoplasmic calcium concentration during fatigue in single mouse muscle fibers. *J Gen Physiol* **98,** 615-635.

Westerblad H & Allen DG. (1992). Changes of intracellular pH due to repetitive stimulation of single fibres from mouse skeletal muscle. *J Physiol* **449,** 49-71.

Westerblad H & Allen DG. (1994). The role of sarcoplasmic reticulum in relaxation of mouse muscle; effects of 2,5-di(tert-butyl)-1,4-benzohydroquinone. *J Physiol* **474,** 291-301.

Whitfield J, Gamu D, Heigenhauser GJF, VAN Loon LJC, Spriet LL, Tupling AR, Holloway GP. (2017). Beetroot Juice Increases Human Muscle Force without Changing Ca^{2+}-Handling Proteins. *Med Sci Sports Exerc*. **49**, 2016-2024.

Whitfield J, Ludzki A, Heigenhauser GJ, Senden JM, Verdijk LB, van Loon LJ, Spriet LL, Holloway GP. (2016). Beetroot juice supplementation reduces whole body oxygen consumption but does not improve indices of mitochondrial efficiency in human skeletal muscle. *J Physiol*. **594,** 421-435.

Wolosker H, Rocha JB, Engelender S, Panizzutti R, De Miranda J, de Meis L. (1997). Sarco/endoplasmic reticulum Ca^{2+}-ATPase isoforms: diverse responses to acidosis. *Biochem J*. **321**, 545-50.

Wylie LJ, Kelly J, Bailey SJ, Blackwell JR, Skiba PF, Winyard PG, Jeukendrup AE, Vanhatalo A, Jones AM. (2013). Beetroot juice and exercise: pharmacodynamic and dose-response relationships. *J Appl Physiol* **115**, 325-336.

Wylie LJ, Park JW, Vanhatalo A, Kadach S, Black MI, Stoyanov Z, Schechter AN, Jones AM, Piknova B. (in press). Human skeletal muscle nitrate store: influence of dietary nitrate supplementation and exercise. *J Physiol*. doi: 10.1113/JP278076.

Yang T, Peleli M, Zollbrecht C, Giulietti A, Terrando N, Lundberg JO, Weitzberg E, Carlström M. (2015). Inorganic nitrite attenuates NADPH oxidase-derived superoxide generation in activated macrophages via a nitric oxide-dependent mechanism. *Free Radic Biol Med* **83**, 159-166.

Zamani P, Rawat D, Shiva-Kumar P, Geraci S, Bhuva R, Konda P, Doulias PT, Ischiropoulos H, Townsend RR, Margulies KB, Cappola TP, Poole DC, Chirinos JA. (2015). Effect of inorganic nitrate on exercise capacity in heart failure with preserved ejection fraction. *Circulation* **131**, 371-80.

Zhu X, Heunks LM, Versteeg EM, van der Heijden HF, Ennen L, van Kuppevelt TH, Vina J, Dekhuijzen PN. (2005). Hypoxia-induced dysfunction of rat diaphragm: role of peroxynitrite. *Am J Physiol Lung Cell Mol Physiol* **288**, 16-26.

Competing interests: No conflicts of interest, financial or otherwise, are declared by the author(s).

Author contributions: S.J.B., P.G.G., A.M.J., M.C.H, and L.N. contributed to the conception, design and interpretation of the data. S.J.B., P.G.G., and L.N. performed the experimental work. S.J.B. and L.N. analysed the data. S.J.B., A.M.J., M.C.H. and L.N. wrote the manuscript. All authors approved the final version of the manuscript.

Funding: This research was supported by the National Institute of Arthritis and Musculoskeletal and Skin Diseases Grant AR-069577 (to M.C.H), the University of Exeter Outward Mobility Academic Fellowship (to S.J.B.), and the Conselho Nacional de Desenvolvimento Científico e Tecnológico (CNPq–Universal no. 424527/2016-2; to L.N.).

FIGURE LEGENDS

Figure 1. Schematic of the experimental protocol.

Figure 2. Effect of sodium nitrite ($NaNO_2$) incubation on fatigue development at supra-physiological (20% O_2, ~156 Torr; Panel A) and near-physiological oxygen tensions (2% O_2, ~15 Torr; Panels B and C) in single skeletal muscle fibres. Panel A illustrates time to task failure during repeated tetanic contractions performed in fibres not loaded with fluorescent probes at a supra-physiological P_{O_2} in the absence (fatigue #1; control) or presence of 100 µM $NaNO_2$ (fatigue #2; n= 4 fibres). Panel B illustrates time to task failure in fibres not loaded with fluorescent probes performed at near-physiological P_{O_2} in the absence and presence of 100 µM $NaNO_2$ (n= 4 fibres). Panel C illustrates time to task failure in all fibres from this study (not loaded and loaded with fluorescent probes) that were performed at near-physiological P_{O_2} in the absence (fatigue #1; control) or presence of 100 µM $NaNO_2$ (fatigue #2; n= 14 fibres). The bars represent group mean data with the lines representing responses in individual muscle fibres. Data are presented as mean ± SD. *P<0.05 vs. fatigue #1.

Figure 3. Sodium nitrite ($NaNO_2$) incubation at a near-physiological oxygen tension (2% O_2, ~15 Torr) does not alter myofibrillar calcium (Ca^{2+}) sensitivity during single evoked non-fatiguing contractions. Panel A illustrates isometric force development in single skeletal muscle fibres evoked by different frequencies of pulse stimulation before fatigue #1 (FF#1) and before fatigue #2 (FF#2; after 1 h incubation with 100 µM $NaNO_2$). Panel B illustrates intracellular cytosolic Ca^{2+} concentration ($[Ca^{2+}]_c$) at rest, contractions at different pulse-frequencies, and at 120 Hz stimulation in the presence of 10 mM caffeine. Panel C plots force development against $[Ca^{2+}]_c$ at each pulse-frequency. *P<0.05 vs. Control. Data (n=5 fibres) are presented as mean ± SD.

Figure 4. Isometric force development and intracellular cytosolic calcium concentration ($[Ca^{2+}]_c$) responses during a repeated fatigue-inducing contraction protocol competed in the absence and presence of sodium nitrite ($NaNO_2$) at a near-physiological oxygen tension (2% O_2, ~15 Torr). Panel A illustrates the peak $[Ca^{2+}]_c$ responses up to the time of task failure.

Panel B illustrates basal $[Ca^{2+}]_c$ data, obtained from the 100 ms period before each contraction, up to the time of task failure (*P<0.05 vs. Control). Note the blunted increase in basal $[Ca^{2+}]_c$ in the $NaNO_2$ condition. Panel C illustrates the change (Δ) in basal $[Ca^{2+}]_c$ from rest to task failure. The $Ca^{2+}{}_{50}$ before and during fatiguing contractions are illustrated in Panel D with group mean responses as bars and individual responses as lines (*P<0.05 vs. FF#1). Data (n=5 fibres) are presented as mean ± SD.

Figure 5. Analysis of sarcoplasmic reticulum calcium (Ca^{2+}) pumping at different time-points during the fatigue-inducing contraction protocols run in the absence and presence of sodium nitrite ($NaNO_2$) at a near-physiological oxygen tension (2% O_2, ~15 Torr). The intracellular cytosolic Ca^{2+} concentration ($[Ca^{2+}]_c$) dependence of the rate of $[Ca^{2+}]_c$ decay ($-d[Ca^{2+}]_c/dt$) during the "tail" of $[Ca^{2+}]_c$ decay is illustrated after the first contraction (Panel A), after 80 s of contractions (Panel B) and the contraction at the time of task failure (Panel C). Note the left shifting of the $NaNO_2$ curve compared to the control curve after 80 s of contractions and at the time of task failure, but not after the first contraction. The changes in SR Ca^{2+} pumping rate at these time-points are presented in Panels D (first contraction), E (after 80 s of contractions), and F (time of task failure). *P<0.05 vs. control. Data (n=5 fibres) are presented as mean ± SD.

Figure 6. Intracellular pH (pH_i) responses during the fatigue-inducing contraction protocols run in the absence and presence of sodium nitrite ($NaNO_2$) at a near-physiological oxygen tension (2% O_2, ~15 Torr). pH_i changes during the repeated fatiguing contractions. *P<0.05 vs. control. †P<0.05 vs initial contraction. Data (n=5 fibres) are presented as mean ± SD.

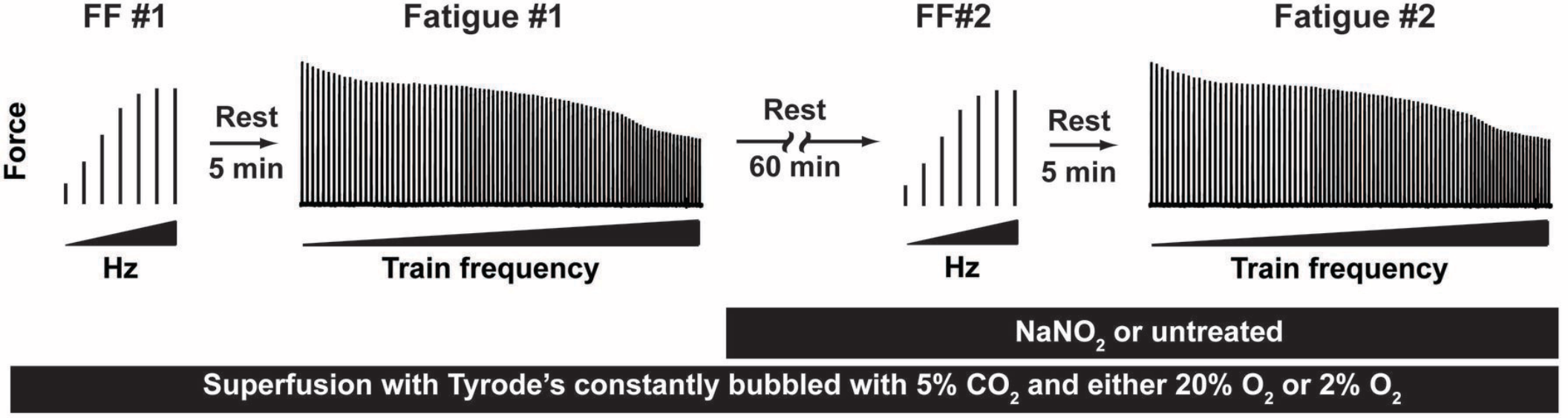
FF #1
Fatigue #1
FF#2
Fatigue #2
Force
Rest
5 min
Rest
60 min
Rest
5 min
Hz
Train frequency
Hz
Train frequency
NaNO2 or untreated
Superfusion with Tyrode's constantly bubbled with 5% CO2 and either 20% O2 or 2% O2

Figure 1

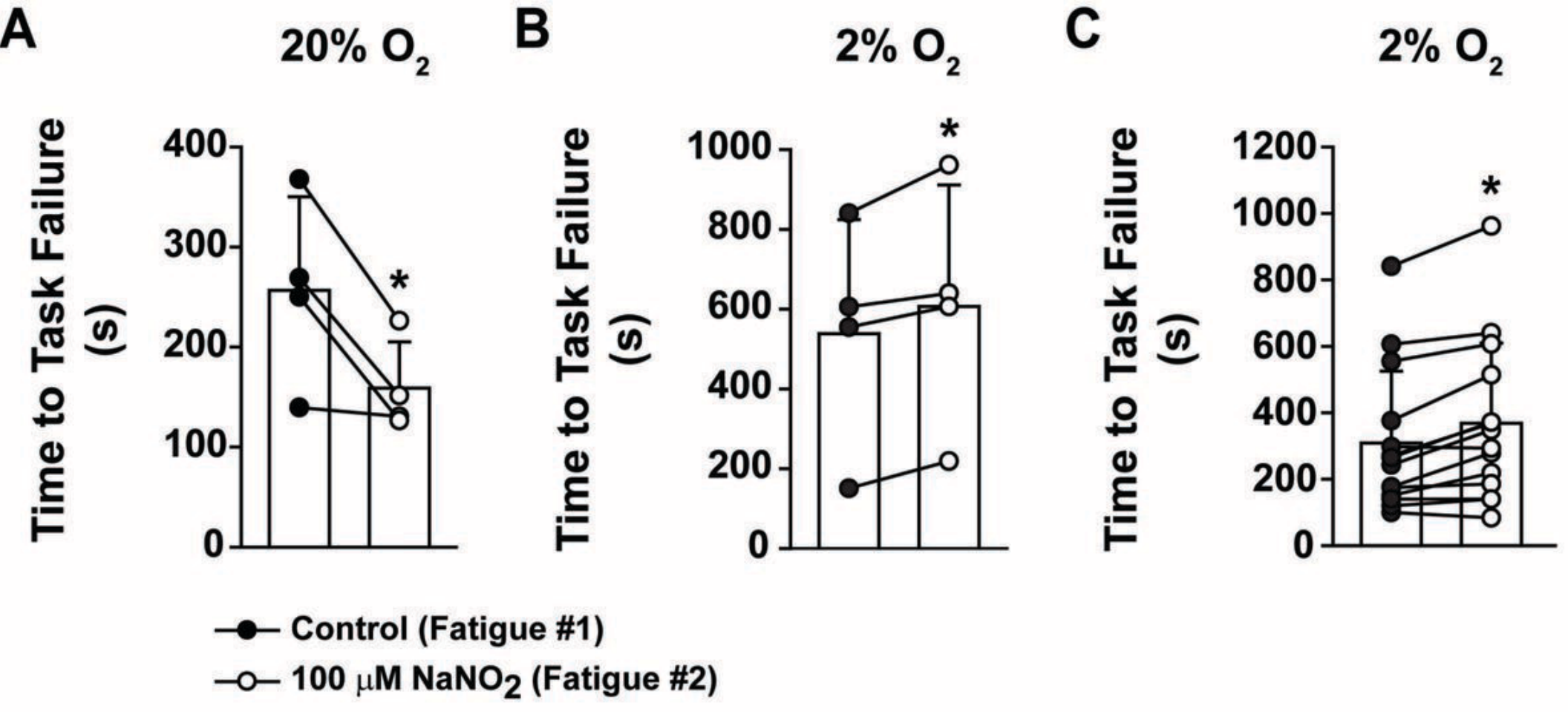
A
20% O_2
Time to Task Failure (s)
400
300
200
100
0
*
B
2% O_2
Time to Task Failure (s)
1000
800
600
400
200
0
*
C
2% O_2
Time to Task Failure (s)
1200
1000
800
600
400
200
0
*
Control (Fatigue #1)
100 μM $NaNO_2$ (Fatigue #2)

Figure 2

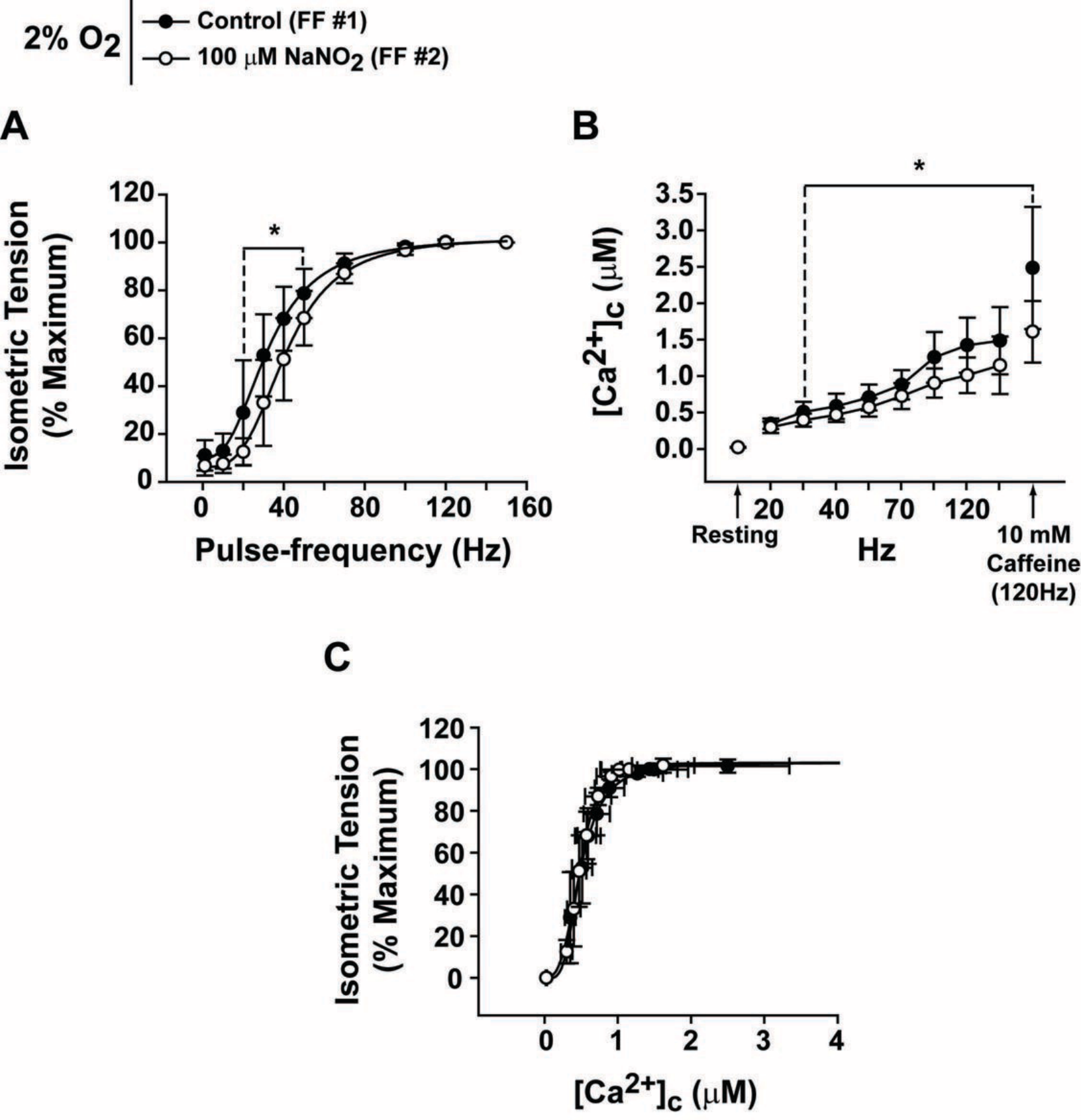
2% O2
Control (FF #1)
100 μM NaNO2 (FF #2)
A
Isometric Tension (% Maximum)
Pulse-frequency (Hz)
B
[Ca2+]c (μM)
Resting
Hz
10 mM Caffeine (120Hz)
C
Isometric Tension (% Maximum)
[Ca2+]c (μM)

Figure 3

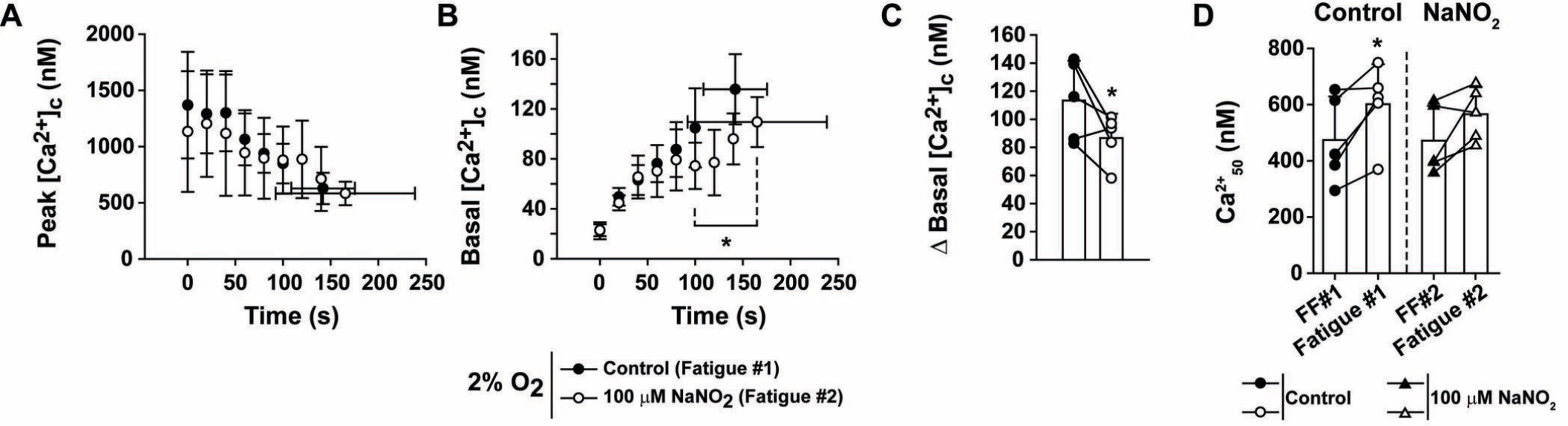
A
Peak [Ca2+]c (nM)
2000
1500
1000
500
0
0 50 100 150 200 250
Time (s)
B
Basal [Ca2+]c (nM)
160
120
80
40
0
*
0 50 100 150 200 250
Time (s)
C
Δ Basal [Ca2+]c (nM)
160
140
120
100
80
60
40
20
0
*
D
Control NaNO2
Ca2+ 50 (nM)
800
600
400
200
0
*
FF#1
Fatigue #1
FF#2
Fatigue #2
2% O2
Control (Fatigue #1)
100 μM NaNO2 (Fatigue #2)
Control
100 μM NaNO2

Figure 4

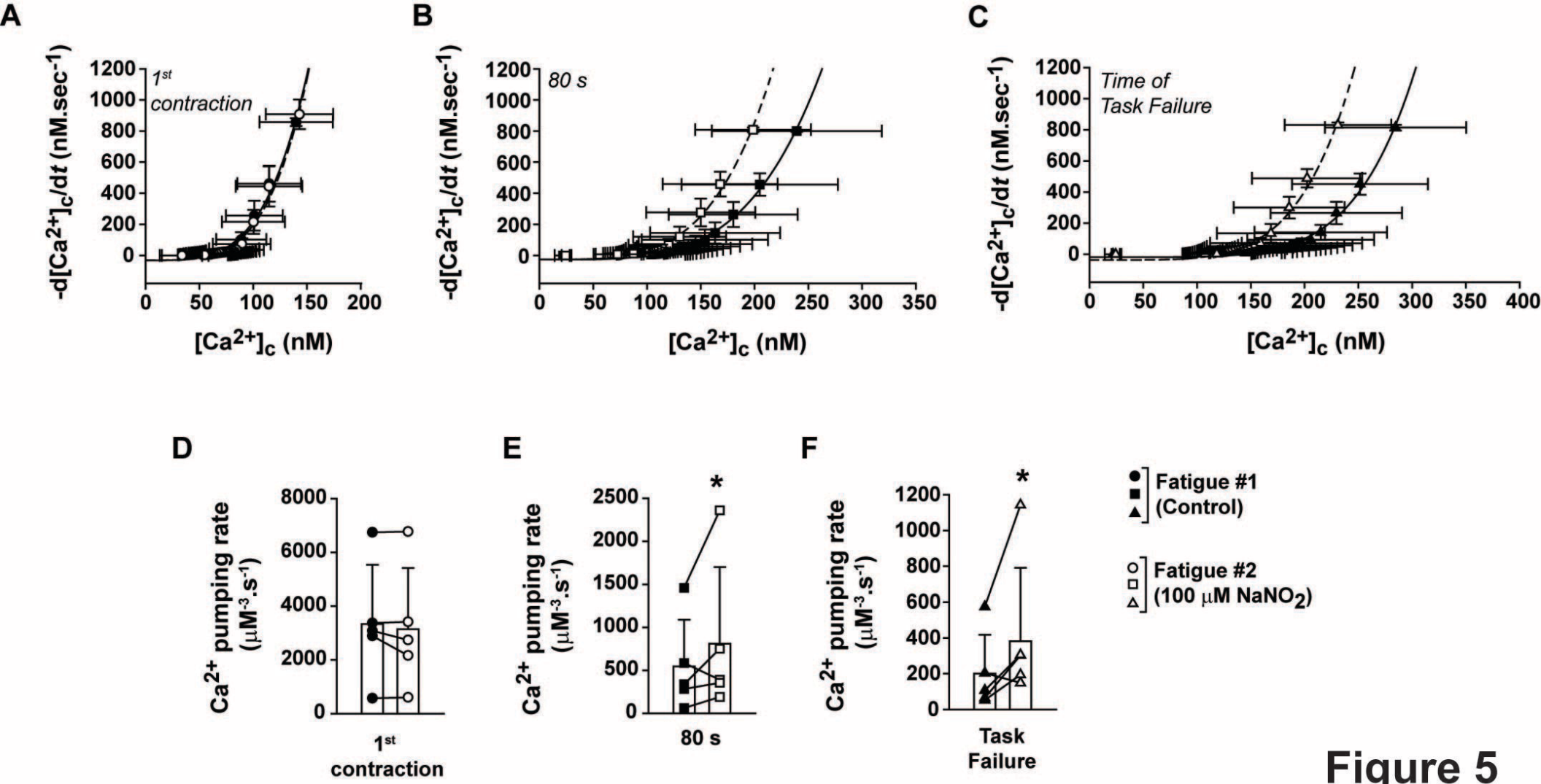
A
B
C
1st contraction
80 s
Time of Task Failure
-d[Ca2+]c/dt (nM.sec-1)
[Ca2+]c (nM)
D
E
F
Ca2+ pumping rate (μM-3.s-1)
1st contraction
80 s
Task Failure
*
Fatigue #1 (Control)
Fatigue #2 (100 μM NaNO2)

Figure 5

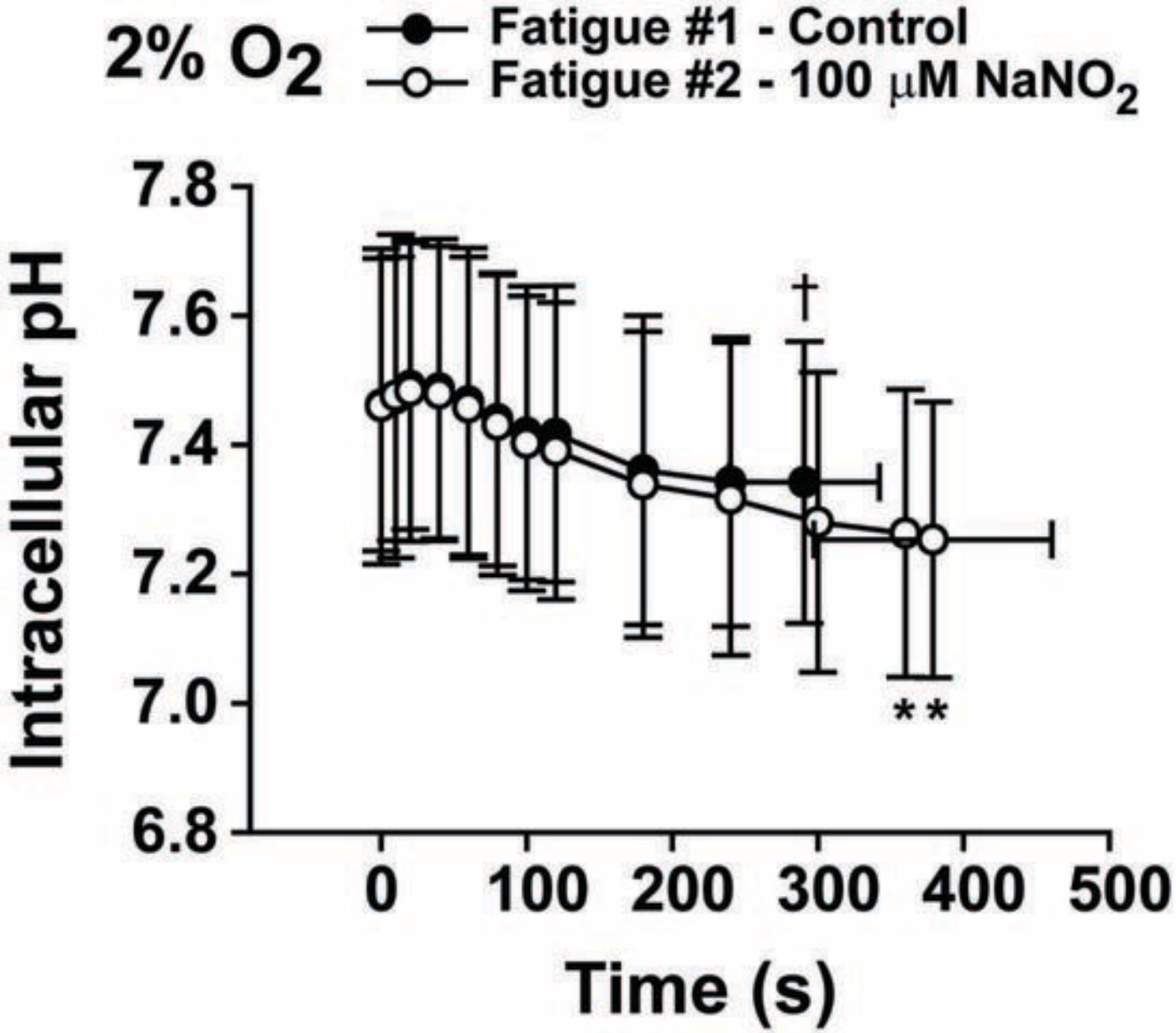
2% O2
Fatigue #1 - Control
Fatigue #2 - 100 μM NaNO2
Intracellular pH
7.8
7.6
7.4
7.2
7.0
6.8
†
**
0
100
200
300
400
500
Time (s)

Figure 6